



Delft University of Technology

## Thermal aging behaviors of the waste tire rubber used in bitumen modification

Wang, Haopeng; Liu, Xueyan; Varveri, Aikaterini; Zhang, Hongzhi; Erkens, Sandra; Skarpas, Athanasios; Leng, Zhen

**DOI**

[10.1177/14777606211038951](https://doi.org/10.1177/14777606211038951)

**Publication date**

2021

**Document Version**

Final published version

**Published in**

Progress in Rubber, Plastics and Recycling Technology

**Citation (APA)**

Wang, H., Liu, X., Varveri, A., Zhang, H., Erkens, S., Skarpas, A., & Leng, Z. (2021). Thermal aging behaviors of the waste tire rubber used in bitumen modification. *Progress in Rubber, Plastics and Recycling Technology*, 38(1), 56-69. <https://doi.org/10.1177/14777606211038951>

**Important note**

To cite this publication, please use the final published version (if applicable).  
Please check the document version above.

**Copyright**

Other than for strictly personal use, it is not permitted to download, forward or distribute the text or part of it, without the consent of the author(s) and/or copyright holder(s), unless the work is under an open content license such as Creative Commons.

**Takedown policy**



Please contact us and provide details if you believe this document breaches copyrights.  
We will remove access to the work immediately and investigate your claim.

# Thermal aging behaviors of the waste tire rubber used in bitumen modification

Progress in Rubber Plastics and  
Recycling Technology  
1–14

© The Author(s) 2021

Article reuse guidelines:  
sagepub.com/journals-permissions  
DOI: 10.1177/14777606211038951  
journals.sagepub.com/home/prp

Haopeng Wang<sup>1,2</sup> , Xueyan Liu<sup>1</sup>,  
Aikaterini Varveri<sup>1</sup> , Hongzhi Zhang<sup>3,4</sup>,  
Sandra Erkens<sup>1</sup>, Athanasios Skarpas<sup>1,5</sup>  
and Zhen Leng<sup>2</sup>

## Abstract

Considering the application scenarios of rubber granules from waste tires in the bitumen modification process (wet or dry process), both aerobic and anaerobic aging of rubber may occur. The current study aims to investigate the thermal aging behavior of waste tire rubber samples using nanoindentation and environment scanning electron microscopy (ESEM) tests. Both aerobic and anaerobic aging tests with different durations were conducted on rubber samples. The complex moduli of aged rubber samples were measured by nanoindentation tests. The surface morphology and elemental composition of aged samples were obtained by ESEM tests together with the energy dispersive X-ray analysis. Results have shown that for both aerobic and anaerobic aging, the equilibrium modulus derived from the complex modulus curve first increases and then decreases with aging time. However, the time needed for the aerobically aged sample to reach the maximum equilibrium modulus is shorter than the anaerobic case. Aging results in crack propagation and an increase of sulfur content on the rubber surface until it reaches the peak. The degree of crosslinking reflected by sulfur content for anaerobic aging is higher than aerobic aging. The morphological change

<sup>1</sup> Section of Pavement Engineering, Faculty of Civil Engineering & Geosciences, Delft University of Technology, Delft, The Netherlands

<sup>2</sup> Department of Civil and Environmental Engineering, The Hong Kong Polytechnic University, Hong Kong, People's Republic of China

<sup>3</sup> Microlab, Faculty of Civil Engineering & Geosciences, Delft University of Technology, Delft, The Netherlands

<sup>4</sup> School of Qilu Transportation, Shandong University, Jinan, People's Republic of China

<sup>5</sup> Department of Civil Infrastructure and Environmental Engineering, Khalifa University, Abu Dhabi, the United Arab Emirates

## Corresponding author:

Haopeng Wang, Section of Pavement Engineering, Faculty of Civil Engineering & Geosciences, Delft University of Technology, Stevinweg 1, 2628 CN, Delft, The Netherlands; Department of Civil and Environmental Engineering, The Hong Kong Polytechnic University, Hong Kong, People's Republic of China.

Email: haopeng.wang@tudelft.nl

and elemental change of rubber correlate well with the change of mechanical properties. The aging of rubber from the waste truck tire at 180°C can generally be separated into two stages: crosslinking dominant stage and chain scission dominant stage.

## Keywords

Waste tire rubber, thermal aging, nanoindentation, viscoelasticity, ESEM, EDX

Received 12 February 2020; accepted 25 June 2021

## Introduction

The significant increase in the number of vehicles around the world has generated approximately one billion waste tires annually.<sup>1</sup> The illegally dumped or stockpiled tires raise concerns about public health and environmental problems.<sup>2</sup> Being aware of the environmental and economic advantages, engineers have attempted to dispose the waste tires in a more sustainable way. From a standpoint of materials science, a tire is composed of elastomeric compounds, textile and metal. Waste tires may be useless to tire manufacturing, but they can become appreciated raw materials for other application scenarios. In transport engineering, bituminous binders modified with rubber granules ground from waste tires has been successfully applied in asphalt pavements several decades ago due to the economic and environmental benefits.<sup>3</sup> There are two primary methods of incorporating the reclaimed rubber granules into hot mix asphalt (HMA), which are generally referred to as dry process and wet process.<sup>3</sup> In the dry process, rubber granules are mixed directly with aggregates prior to introducing the hot binder at around 180°C during the HMA production. The rubber particles act as a partial replacement of stone aggregates in asphalt mixtures. Through the wet process, rubber granules are blended with bitumen at a temperature of 160 ~ 220°C and predetermined reaction time is required before mixing the modified binder with aggregates. Considering the normally experienced temperature of tire rubber on the road is lower than 100°C,<sup>4</sup> the processing temperature of rubber-modified bitumen is very high. Therefore, the recycled rubber granules will definitely undergo aging at such a high temperature, which in turn influences the properties of rubber-modified bitumen. In previous studies of rubber-modified bituminous materials,<sup>5-7</sup> efforts were mainly emphasized on the performance evaluation of the blend system of rubber and bitumen. Very limited studies have been done to investigate the thermal aging behavior of rubber particles/granulates at a relatively high temperature.<sup>8-10</sup> Considering the application scenarios of rubber granules in the bitumen modification process, both aerobic and anaerobic aging of rubber may occur. When rubber particles are immersed in the hot bitumen, mainly anaerobic aging of rubber takes place. However, the air is inevitably involved during the mixing process if no extra measures are taken, which causes the aerobic or oxidative aging of rubber.<sup>6,11</sup> A better understanding of the aging mechanism of rubber during the preparation stage of rubberized bituminous materials has two benefits: it can help (i) optimize the processing conditions during bitumen modification; and (ii) predict the performance evolution of rubberized bituminous materials during the service stage of asphalt pavements (e.g., aging).

The present study aims to investigate the thermal aging behavior of waste tire rubber samples with both mechanical and morphological characterization methods. Rubber sheet samples were aged in

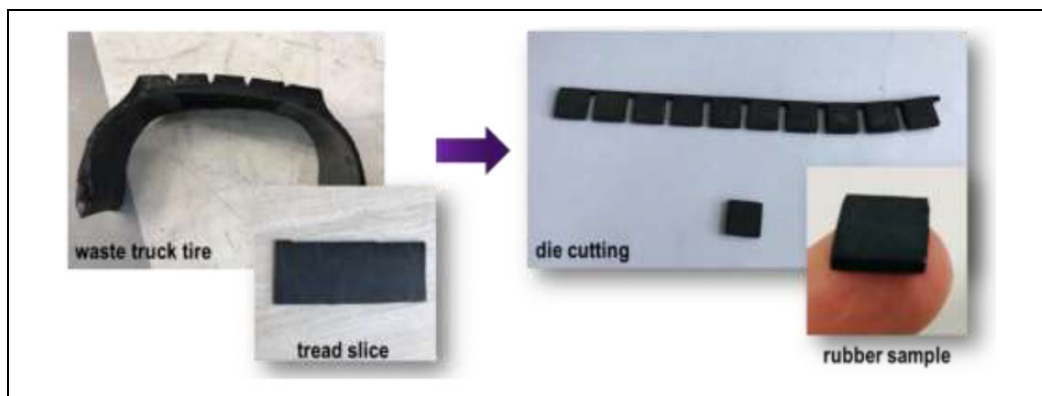


**Figure 1.** Square rubber sample preparation process (dimension:  $10 \times 10 \times 2$  mm).

**Table 1.** Basic properties and composition of the rubber sample.

Properties	Description or value
Source	Scrap truck tire tread
Color	Black
Density ( $\text{g/cm}^3$ )	1.15
Decomposition temperature ( $^{\circ}\text{C}$ )	$\sim 200$
Total rubber (natural and synthetic)	55
Carbon Black (%)	30
Sulfur (%)	1
Zinc oxide (%)	1.5
Benzene extract (%)	5.5
Ash content (%)	7

the oven in both aerobic and anaerobic conditions. Nanoindentation tests and environmental scanning electron microscopy (ESEM) tests were carried out on the aged rubber samples to investigate the aging mechanism.

## Materials and methods

### *Rubber samples*

From the waste truck tire tread, which is metal and fiber free, a uniform rubber sheet of 2 mm thickness was cut using waterjet cutting. Then, die-cutting was adopted to obtain square rubber blocks with a width of 10 mm from the rubber sheet as shown in Figure 1. The detailed technical information of rubber samples is summarized in Table 1.

### *Aging procedure*

The cut rubber piece samples were divided into two groups. One group of rubber samples were put into small glass bottles filled with nitrogen and sealed with lids to create anaerobic conditions. The other group does not need extra treatment as aging was performed in the presence of oxygen

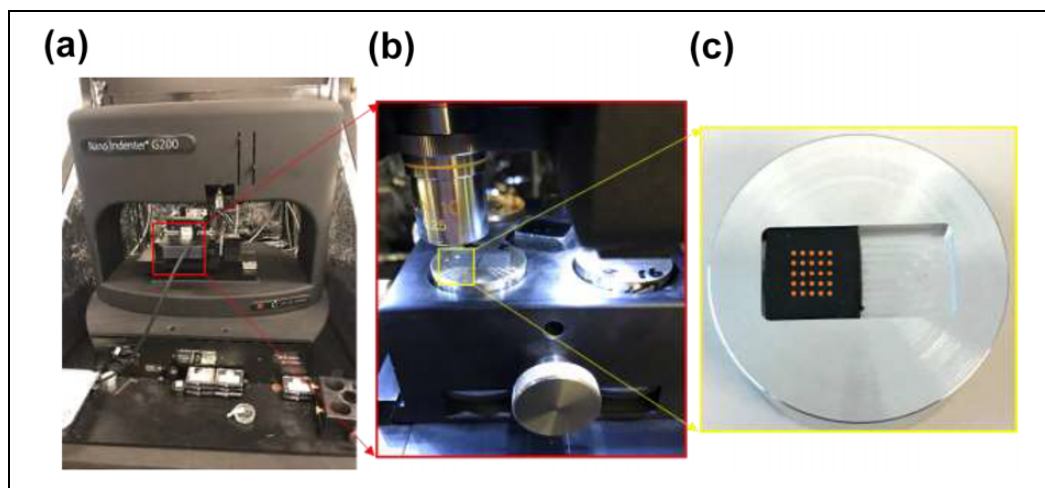


**Figure 2.** Nanoindentation test setup. (a) Nano Indenter G200. (b) Operational platform. (c) Sample holder and measuring points.

(aerobic conditions). The two groups of rubber samples were aged for varying durations in an air circulating oven at 180°C, which is the temperature typically used for mixing rubber and bitumen to prepare rubber-modified binders. Both groups of samples were aged under the same temperature and for the same time in different oxygen environment, i.e. anaerobic aging and aerobic aging (oxidative aging). After 2 h, 4 h, 6 h, 8 h, 16 h, 24 h, and 32 h of oven aging, the rubber samples were subjected to nanoindentation and ESEM tests. Both the mechanical properties and morphological characteristics of the aged rubber samples were investigated and compared with the fresh rubber sample from the waste truck tire tread.

### **Nanoindentation test**

A KLA Nano Indenter G200 as shown in Figure 2 was used for testing the mechanical properties of rubber samples. The continuous stiffness method (CSM) was adopted to measure the complex modulus of samples. This method involves applying a small dynamic load at a certain frequency on the top of a static load while loading. The combination of dynamic and static loads offers a way to separate the in-phase and out-of-phase components of the load-displacement history.<sup>12</sup> The used indenter tip is a flat-ended cylindrical punch made of diamond with a diameter of 330  $\mu\text{m}$ . In view of the higher surface roughness and lower hardness of the rubber samples (compared for example to metals), a flat-ended punch was used as the tip for this test to ensure that the contact area is constant, and not a function of contact depth. As it can be seen in Figure 2(b), the affiliated microscope was used for positioning of the measuring points. In total, 25 indentations at 25 different sites (a  $5 \times 5$  square matrix in Figure 2(c)) were conducted on each sample to deal with the data variability. The interval between these points was 500  $\mu\text{m}$  to eliminate the effects of residual stresses and indenting deformations. The indenter was first brought into full contact with the test material at an approach velocity of 0.05  $\mu\text{m/s}$ . A pre-test compression of 5  $\mu\text{m}$  was applied after detecting the contact. Then the indenter oscillated over a frequency range from 1 ~ 45 Hz and the measuring system recorded the material responses. The harmonic oscillation amplitude was

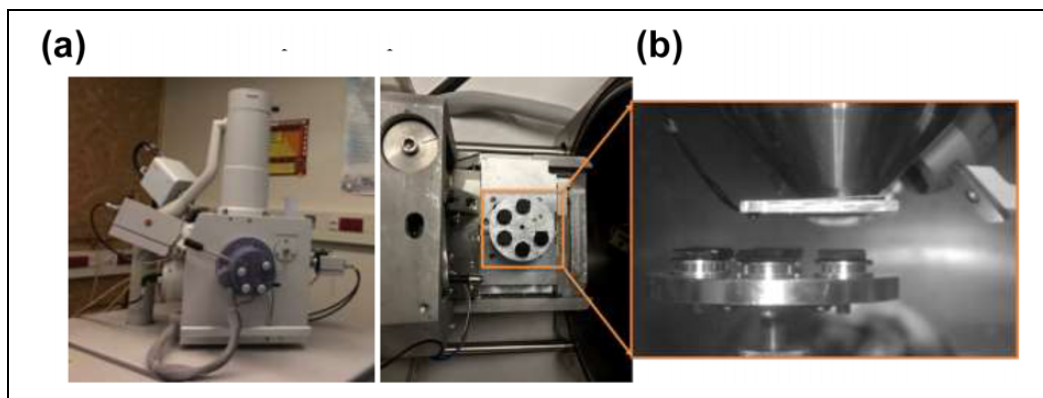


**Figure 3.** ESEM setup (a) exterior (b) rubber samples on the rotatable stage in the chamber.

0.05  $\mu\text{m}$ . After that, the indenter was withdrawn and moved to the next test site. All the indentation tests were performed at 20°C. After obtaining the load-displacement curves, analysis was done to calculate the complex modulus and phase angle as a function of frequency for a specific test site.

### *ESEM with EDX analysis*

The morphological analysis of rubber samples was conducted by a Philips XL30 ESEM with an energy dispersive X-ray spectroscopy (EDX) (Figure 3). To mount the rubber sample on the sample holder, double-sided adhesive tape was used. In total six holders with samples on them can be placed on a rotatable stage in the chamber to be tested one by one. The setting parameters for the observations were as follows<sup>6</sup>:

- chamber pressure: 1 Torr in low vacuum mode
- temperature: 0°C
- acceleration voltage: 20 keV
- spot size: 5.0 nm
- magnification: 100×
- mode: backscattered electron (BSE) mode.

The electron gun was maintained 10 mm above the sample surface. Following the ESEM image capturing, an EDX system was used to conduct the elemental analysis at selected spots on the micrograph to create elemental composition maps with software.

## **Results and discussion**

### *Nanoindentation tests*

The load applied on the sample and the displacement into the sample surface versus time during the nanoindentation tests are presented in Figure 4. Initially, a pre-load was applied to achieve a full contact between the sample surface and the flat punch face. A short stabilization period was imposed to ensure the contact to reach the equilibrium state. Then, a step-load was applied on the sample to evaluate the creep behavior. After that, frequency sweep tests starting from low

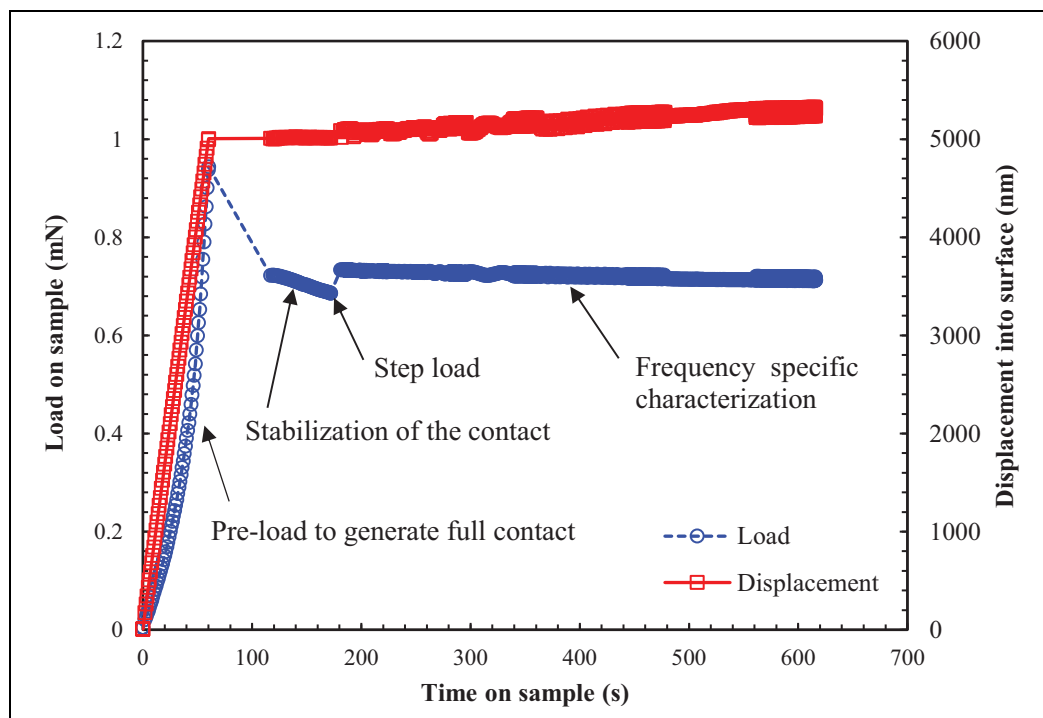


**Figure 4.** A complete indentation test to obtain the complex modulus.

frequency to high frequency were conducted. The combined response of the instrument (oscillator) and the sample as well as the sole response of the oscillator in free space were measured in the frequency domain with a phase-lock amplifier (PLA) in the indentation system. The material response was determined by deducting the instrument's contribution to the total measured response<sup>13</sup> and the mechanical parameters were then calculated with the known stiffness, damping factor, and mass of the instrument. The resulted storage modulus and loss factor as a function of frequency are presented in Figure 5. Each data point represents an average of 25 measurements and the error bar covers the data range with the mean value in the middle. The percent deviation is generally around 10%, which is acceptable for nanoindentation tests. Although rubber is normally treated as an elastic material, the results in Figure 5 clearly show the viscoelastic nature of the waste truck tire rubber. This is evident by the fact that both storage modulus and loss factor increase with frequency in the testing range.

To investigate how thermal aging affects the mechanical properties of waste tire rubber, nanoindentation tests were conducted on both oxidative-aged and anaerobic-aged rubber samples with different aging durations. The complex modulus data for both cases are shown in Figure 6. For the samples aged at aerobic conditions, the nanoindentation tests stopped after 16 h aging. This is because the sample severely cracked after this aging time; more details will be given in the next sub-section where the morphological changes of rubber samples from ESEM tests will be observed. Figure 6 illustrates that for both oxidative and anaerobic aging, the complex modulus first increased and then decreased with aging time. However, the timings for the aged sample to

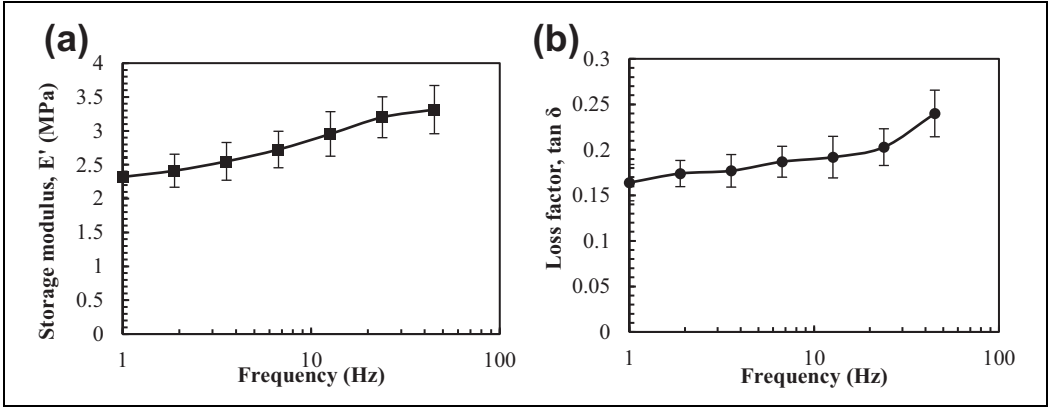


**Figure 5.** (a) Storage modulus  $E'$  and (b) loss factor  $\tan \delta$  versus frequency of the unaged rubber sample.

reach the maximum complex modulus are different for oxidative and anaerobic aging. Different aging mechanisms are accounted for this difference, which will be elaborated later in this section.

To demonstrate the effects of thermal aging on the viscoelastic properties of waste tire rubber more explicitly, the viscoelastic behavior was represented by the generalized Maxwell (GM) model.<sup>14,15</sup> The GM model is the most general form of the linear model for viscoelasticity. It has been widely used for modeling the viscoelastic behaviors of rubber materials.<sup>16,17</sup> This mechanistic model comprises a spring unit and  $n$  Maxwell elements connected in parallel. The relaxation modulus  $E_r$  in the time domain and the complex modulus  $E^*$  in the frequency domain are respectively given by equations (1) and (2).

$$E_r(t) = E_\infty + \sum_{i=1}^n E_i e^{-\frac{t}{\rho_i}} \quad (1)$$

$$E^*(\omega) = E'(\omega) + iE''(\omega) = \left( E_\infty + \sum_{j=1}^n \frac{\omega^2 \rho_j^2 E_j}{1 + \omega^2 \rho_j^2} \right) + i \sum_{j=1}^n \frac{\omega \rho_j E_j}{1 + \omega^2 \rho_j^2} \quad (2)$$

where  $E_\infty$  is the equilibrium modulus, at infinite loading time;  $E_i$  is the relaxation strength;  $\rho_i$  is the relaxation time;  $t$  is the loading time;  $\omega$  is the loading frequency. The representation of the relaxation modulus by the GM model is commonly known as the Prony series. The Prony coefficients ( $E_\infty$ ,  $E_i$ ,  $\rho_i$ ) were obtained by statistically fitting on experimental data by minimizing the following objective function.<sup>18</sup>

$$f_{\min} = \sum_{j=1}^n \left[ \left( \frac{E'(\omega_j)_f}{E'(\omega_j)_e} - 1 \right)^2 + \left( \frac{E''(\omega_j)_f}{E''(\omega_j)_e} - 1 \right)^2 \right] \quad (3)$$

where  $E'(\omega_j)_f$  and  $E''(\omega_j)_f$  are fitted storage and loss modulus at frequency  $\omega_j$ ;  $E'(\omega_j)_e$  and  $E''(\omega_j)_e$  are experimental storage and loss modulus at frequency  $\omega_j$ . Figure 7 presents the comparison between experimental data and fitted data using the generalized Maxwell model with four branches. It can be seen for both storage and loss modulus, the fitted data correlates well with the experimental data. Table 2 summarizes the Prony series coefficients of rubber samples at



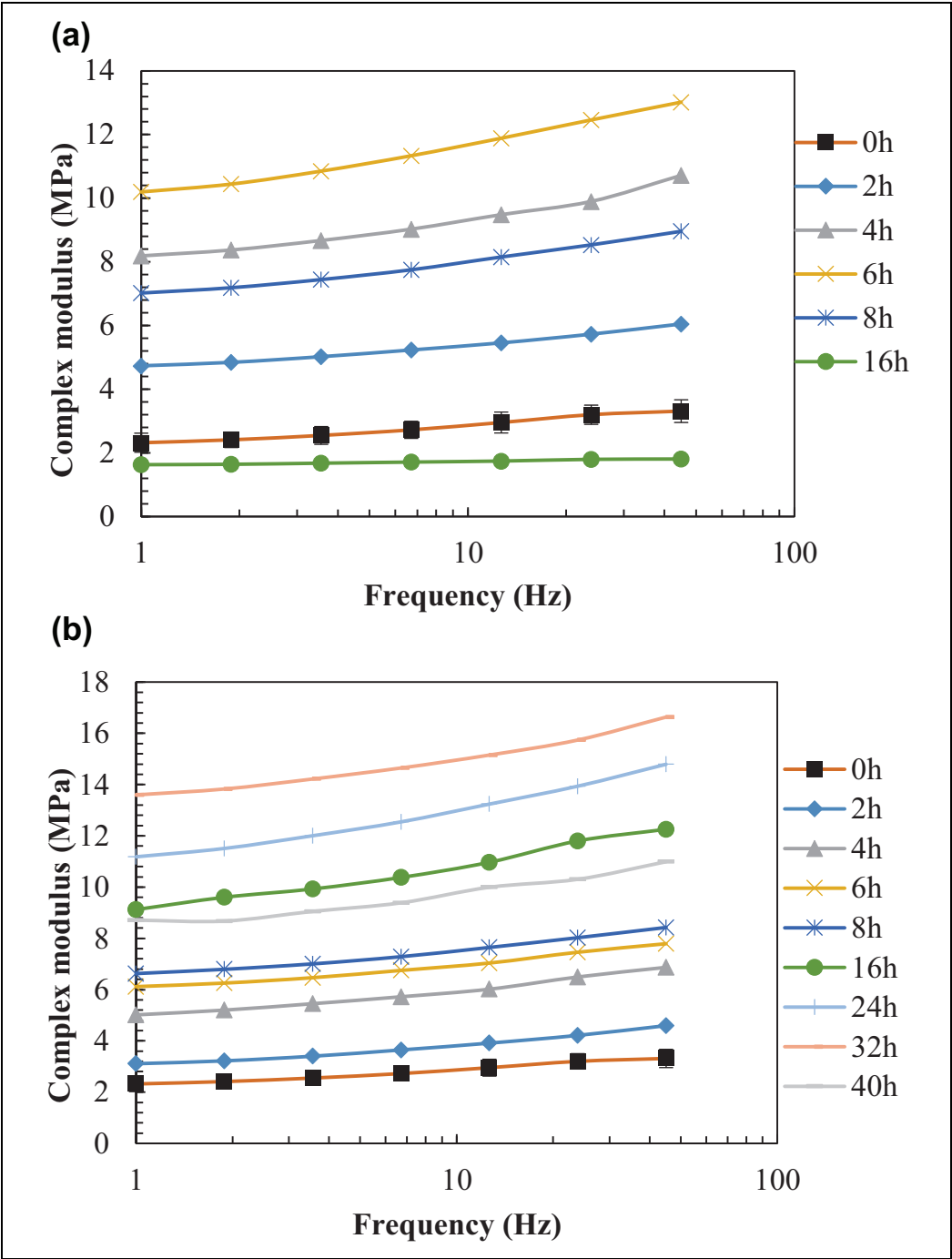


**Figure 6.** Complex modulus versus frequency of aged rubber samples with different aging durations (a) aerobic condition (b) anaerobic condition.

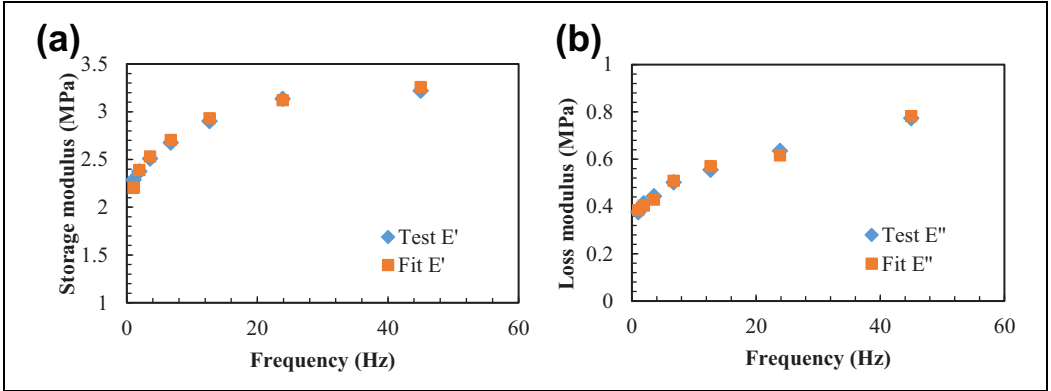


**Figure 7.** Experimental data versus generalized Maxwell model fitted data of the unaged sample (a) storage modulus (b) loss modulus.

**Table 2.** Prony coefficients of rubber samples at different aging states.

Aging state	Prony coefficients								
	$E_{\infty}$ (MPa)	$E_1$ (MPa)	$\rho_1$ (s)	$E_2$ (MPa)	$\rho_2$ (s)	$E_3$ (MPa)	$\rho_3$ (s)	$E_4$ (MPa)	$\rho_4$ (s)
Unaged	1.897	10.074	0.001	0.451	0.01	0.699	0.1	0.602	1
Aerobic-2 h	4.054	0	0.001	1.651	0.01	0.833	0.1	0.921	1
Aerobic-4 h	7.268	0	0.001	2.641	0.01	1.386	0.1	1.365	1
Aerobic-6 h	9.068	0	0.001	3.258	0.01	1.844	0.1	1.649	1
Aerobic-8 h	6.236	0	0.001	2.320	0.01	1.190	0.1	1.150	1
Aerobic-16 h	1.516	0	0.001	0.303	0.01	0.149	0.1	0.143	1
Anaerobic-2 h	2.592	0	0.001	1.694	0.01	0.863	0.1	0.758	1
Anaerobic-4 h	4.381	0	0.001	2.191	0.01	1.157	0.1	0.950	1
Anaerobic-6 h	5.203	0	0.001	2.325	0.01	1.105	0.1	1.201	1
Anaerobic-8 h	5.423	0	0.001	2.452	0.01	1.237	0.1	1.359	1
Anaerobic-16 h	7.961	0	0.001	1.905	0.01	2.268	0.1	1.496	1
Anaerobic-24 h	9.955	0	0.001	3.810	0.01	2.107	0.1	1.923	1
Anaerobic-32 h	12.545	0	0.001	3.105	0.01	1.537	0.1	1.683	1
Anaerobic-40 h	7.210	18.815	0.001	0	0.01	0	0.1	2.497	1

different aging states using the collocation method. It can be seen that a four-branch Prony series is sufficient to simulate the complete relaxation behavior of rubber as most of the values of  $E_1$  equal to zero. Furthermore, all rubber samples show an equilibrium modulus at an infinite loading time when the whole stress is born by the separate spring. The equilibrium modulus is essentially an elastic modulus that is attributable to the strong polymer network of rubber. For tire rubber, its network structure mainly comes from the polymer chains and crosslinks.<sup>19</sup> Therefore, the effects of thermal aging on the change of network structure of rubber can be reflected by monitoring the change of equilibrium modulus.

The variation of the equilibrium modulus of rubber after different aging durations is plotted in Figure 8. For aerobic conditions, the equilibrium modulus initially increased with aging time till 6 h. The peak equilibrium modulus was 9.068 MPa. After that, the equilibrium modulus started to

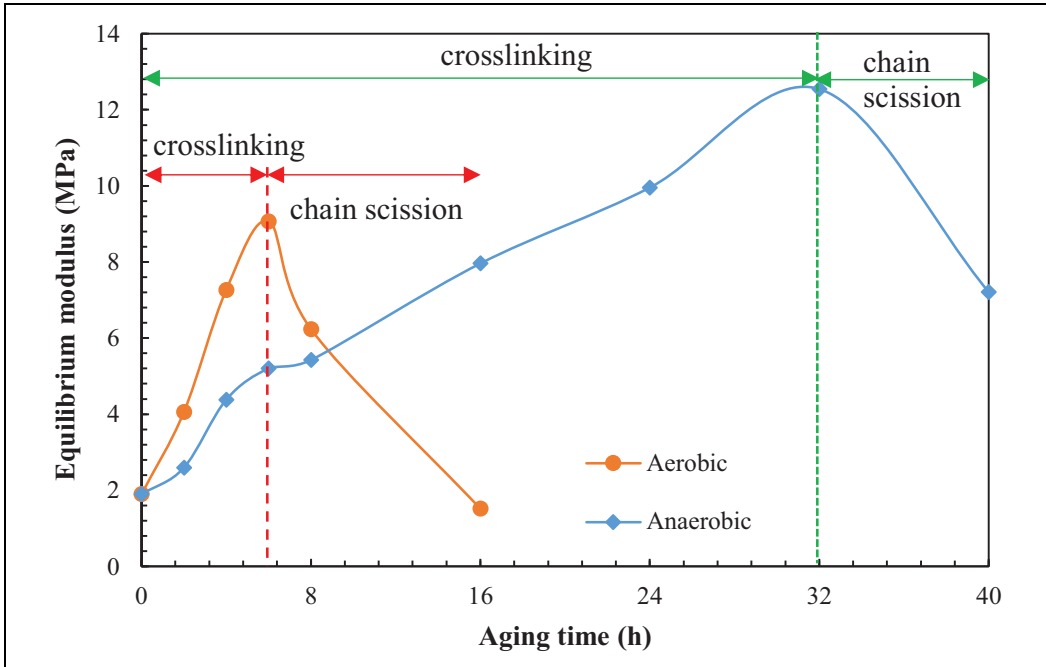


**Figure 8.** Variation of equilibrium modulus of rubber after different aging durations.

decrease with extended aging time. For anaerobic conditions, the equilibrium modulus showed similar trends. However, the transition point at which a change in the equilibrium modulus curve is observed was reached later at 32 h. In addition, the maximum equilibrium modulus was 12.545 MPa, which is higher than the aerobic case. The difference between aerobic and anaerobic aging is due to the different dominant mechanisms. The theory of rubber elasticity shows that the modulus is proportional to the crosslink density of rubber.<sup>20</sup> Therefore, the initial increase in equilibrium modulus is mainly due to the crosslinking of the rubber where the remaining uncrosslinked rubber and curatives allow this reaction to happen under such a high temperature.<sup>21</sup> Simultaneously, the chain scission also takes place under severe conditions. When the chain-scission reaction prevails over the crosslinking reaction, the equilibrium modulus will show a downtrend. It is noteworthy that crosslinking and chain scission occur simultaneously. Whether the equilibrium modulus increases or decreases is determined by the dominant reaction. For aerobic conditions, the presence of oxygen accelerates the chain-scission reaction. At high temperatures, the rate of chain scission becomes appreciable and eventually exceeds the rate of crosslinking under the attack of oxygen, which advances the deterioration of mechanical properties. Furthermore, under anaerobic conditions, the rubber undergoes fewer chain-scission reactions during the initial stage due to the absence of oxygen. Therefore, the maximum equilibrium modulus it can reach is higher than the aerobic case.

### ESEM tests

To investigate the effect of aging on the morphological change of rubber samples, ESEM tests were conducted on the rubber samples with different aging states. Figure 9 summarizes the

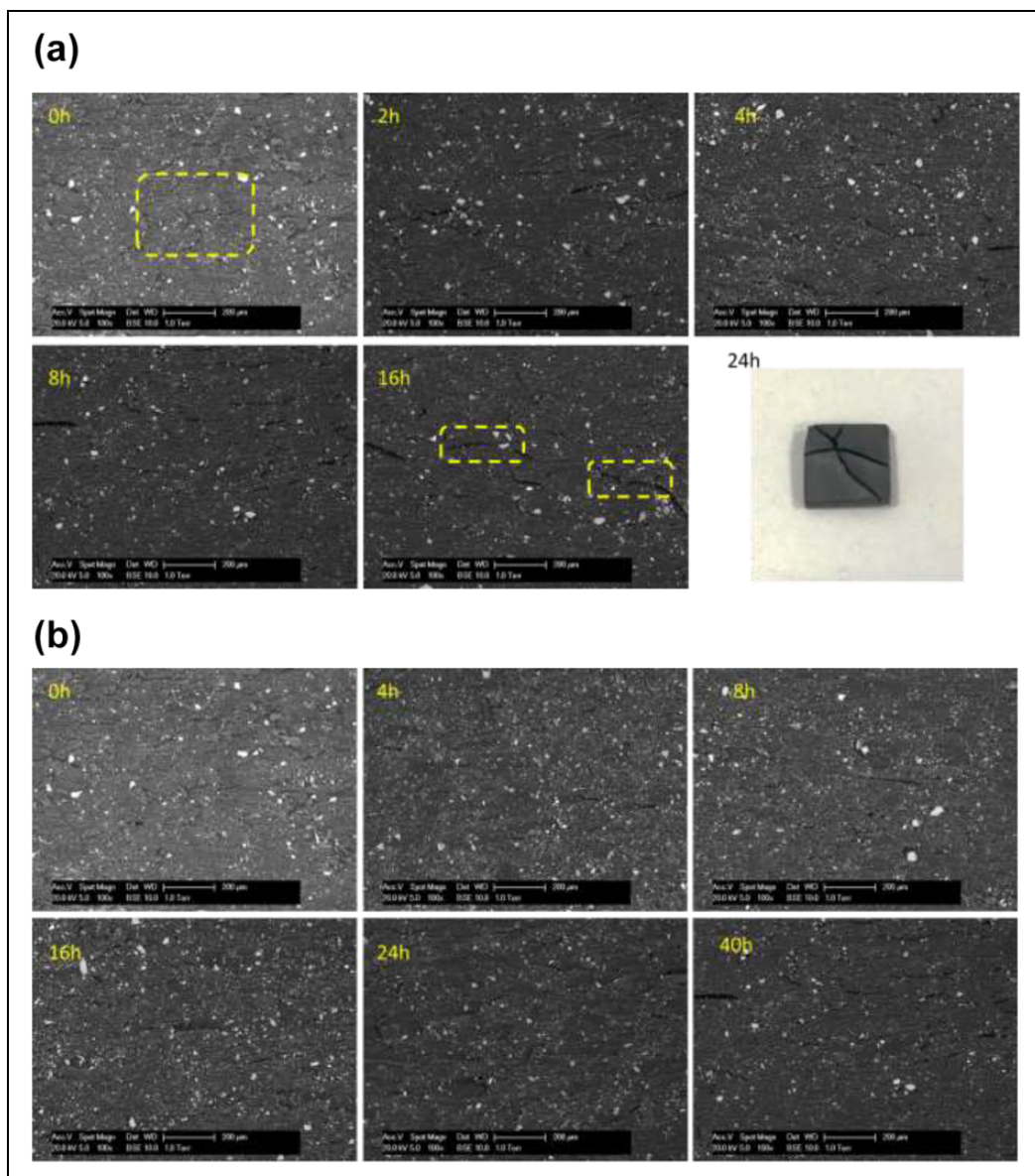


**Figure 9.** ESEM micrographs of rubber surface at different aging states. (a) aerobic condition (b) anaerobic condition.

micrographs of rubber surfaces. The original rubber sample has a ravine-like surface as highlighted in the figure. After aging, the sample surface looks more “glassy” than the unaged one. When increasing the aging time, the original dents are enhanced, and some small cracks appear. It can be clearly seen that the crack size increases after 16 h of aerobic aging in Figure 9(a). A more rugged surface was also observed. This is due to the occurrence of chain scission. After 24 h aerobic aging,

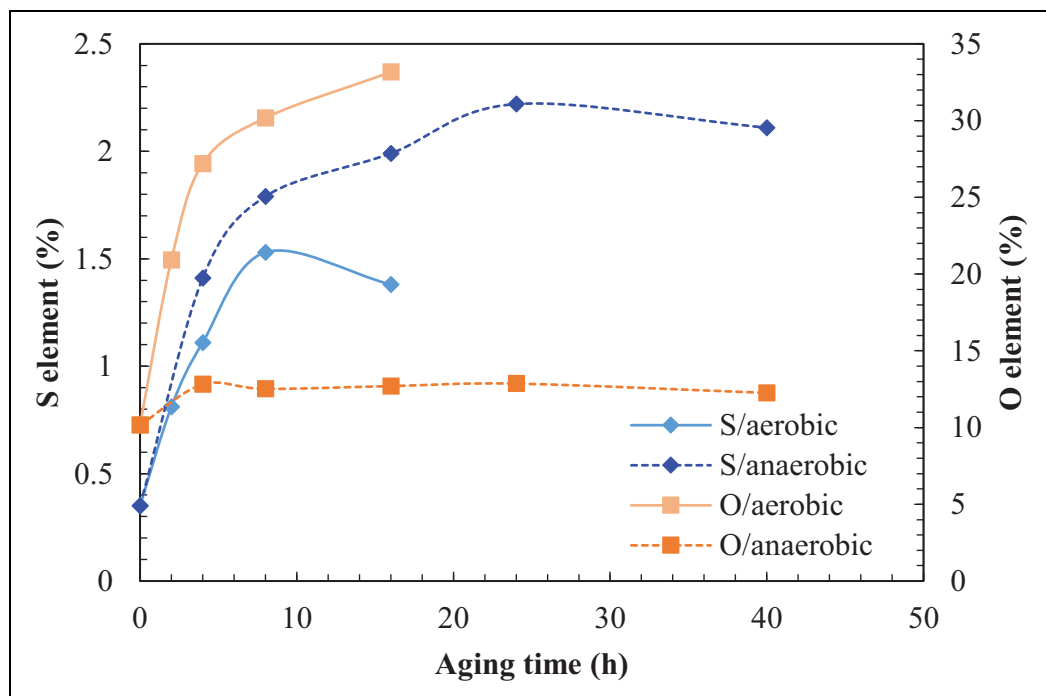


**Figure 10.** Changes in sulfur and oxygen contents with aging time from EDX results.

the rubber sample broke into parts because of the propagation of the cracks. For anaerobic conditions, similar appearance of rubber surface was observed with longer aging time. The whole process seems delayed. After 40 h anaerobic aging, the cracks were still less obvious than the aerobic case of 16 h.

The chemical elements of the rubber surface after aging were analyzed by the EDX system. The sulfur and oxygen elements are of interest because they are related to the aging mechanism. The changes in sulfur and oxygen contents with aging are shown in Figure 10. For aerobic conditions, the content of oxygen kept increasing, which is understandable because of the continuous ingestion of oxygen. The content of sulfur first increased and then decreased. This coincides with initial crosslink process and later chain scission process which breaks the S-S bond in the rubber. By contrast, for anaerobic conditions, the content of oxygen only increased a little bit at the initial stage because of the limited oxygen remaining in the bottle. Then, the content of oxygen was maintained at a similar level. The content of sulfur experienced similar trends as under the aerobic conditions. It only stopped increasing until after around 24 h aging. In addition, the increase of sulfur content after anaerobic aging is higher than that after aerobic aging. This is because there were less chain scission reactions competing with crosslinking reactions due to the absence of oxygen under anaerobic conditions. The degree of crosslinking for anaerobic aging is higher than aerobic aging. From the above analysis, it can be found the morphological and elemental change of rubber from ESEM tests correlate well with the change of mechanical properties from nanoindentation tests. The findings in morphology and element support the conclusions drawn from mechanical test results.

## Conclusions and recommendations

This study investigated the thermal aging behavior of waste tire rubber samples using nanoindentation and ESEM tests. Both aerobic and anaerobic aging tests with different durations were conducted on rubber samples. Detailed sample preparation and experimental procedure were proposed for measuring the viscoelastic parameters of the rubber sample using nanoindentation tests. Key findings from the experimental results are summarized as follows:

1. For both oxidative aging and anaerobic aging, the equilibrium modulus derived from the complex modulus curve first increases with aging time and then decreases. The time needed for the aerobically aged sample to reach the maximum equilibrium modulus is shorter than the anaerobic case.
2. With the increase of aging time, the original dents on the rubber surface are enhanced and some small cracks appear. For aerobic conditions, cracks propagate quickly with aging time, resulting in a breakage of samples after 24 h. For anaerobic conditions, the growth speed of cracks is slower than aerobic conditions due to the absence of oxygen.
3. For both aerobic and anaerobic aging, the content of sulfur on the rubber surface keeps increasing with aging time until it reaches the peak value. The increase and decrease of sulfur content correspond to two different reactions during rubber aging: crosslinking and chain scission. The degree of crosslinking for anaerobic aging is higher than aerobic aging.
4. The morphological change and elemental change of rubber from ESEM tests correlate well with the change of mechanical properties from nanoindentation tests. The aging of rubber from the waste truck tire at 180°C can generally be separated into two stages: crosslinking dominant stage and chain scission dominant stage. Aerobic aging can be considered as an accelerated and intensified process of anaerobic aging. The former reaches the chain scission dominant stage earlier than the latter.

For future studies, aging tests on rubber can be done at various temperatures with extended material combinations. The findings in this study can be used to optimize the mixing temperature and time for preparing rubber modified bitumen to obtain desired binder properties. Furthermore, understanding the thermal aging behaviors of rubber helps to understand the role of rubber in the aging process of rubber modified bitumen and its aging mechanism.

## Declaration of conflicting interests


The author(s) declared no potential conflicts of interest with respect to the research, authorship, and/or publication of this article.

## Funding

The author(s) disclosed receipt of the following financial support for the research, authorship, and/or publication of this article: The corresponding author thanks the financial support from CSC (China Scholarship Council). The financial support from the CIRA-2018-115 research grant of Khalifa University is also gratefully acknowledged.

## ORCID iDs

Haopeng Wang  <https://orcid.org/0000-0002-5008-7322>

Aikaterini Varveri  <https://orcid.org/0000-0002-8830-9437>

## References

1. WBCSD. *End-of-life tires: a framework for effective management systems*. Conches-Geneva, Switzerland: World Business Council for Sustainable Development, 2010.
2. Stevenson K, Stallwood B and Hart AG. Tire rubber recycling and bioremediation: a review. *Bioremediat J* 2008; 12: 1–11.
3. Lo Presti D. Recycled tyre rubber modified bitumens for road asphalt mixtures: a literature review. *Constr Build Mater* 2013; 49: 863–881.
4. Huang D, LaCount BJ, Castro JM, et al. Development of a service-simulating, accelerated aging test method for exterior tire rubber compounds I. Cyclic aging. *Polym Degrad Stabil* 2001; 74: 353–362.
5. Wang H, Liu X, Zhang H, et al. Micromechanical modelling of complex shear modulus of crumb rubber modified bitumen. *Mater Des* 2020; 188: 108467.
6. Wang H, Liu X, Zhang H, et al. Asphalt-rubber interaction and performance evaluation of rubberised asphalt binders containing non-foaming warm-mix additives. *Road Mater Pavement Des* 2020; 21: 1612–1633.
7. Wang H, Zhang H, Liu X, et al. Micromechanics-based complex modulus prediction of crumb rubber modified bitumen considering interparticle interactions. *Road Mater Pavement Des* 2021; 22: 1–18.
8. Baldwin JM and Bauer DR. Rubber oxidation and tire aging-a review. *Rubber Chem Technol* 2008; 81: 338–358.
9. Liu J, Li X, Xu L, et al. Investigation of aging behavior and mechanism of nitrile-butadiene rubber (NBR) in the accelerated thermal aging environment. *Polym Test* 2016; 54: 59–66.
10. Nadal Gisbert A, Crespo Amorós JE, López Martínez J, et al. Study of thermal degradation kinetics of elastomeric powder (ground tire rubber). *Polym Plast Technol Eng* 2007; 47: 36–39.
11. Leng Z, Yu H, Zhang Z, et al. Optimizing the mixing procedure of warm asphalt rubber with wax-based additives through mechanism investigation and performance characterization. *Constr Build Mater* 2017; 144: 291–299.
12. Li XD and Bhushan B. A review of nanoindentation continuous stiffness measurement technique and its applications. *Mater Charact* 2002; 48: 11–36.
13. Herbert EG, Oliver WC and Pharr GM. Nanoindentation and the dynamic characterization of viscoelastic solids. *J Phys D Appl Phys* 2008; 41: 074021.
14. Park SW and Schapery RA. Methods of interconversion between linear viscoelastic material functions. Part I - a numerical method based on Prony series. *Int J Solids Struct* 1999; 36: 1653–1675.
15. Lu GY, Wang HP, Zhang YQ, et al. The hydro-mechanical interaction in novel polyurethane-bound pervious pavement by considering the saturation states in unbound granular base course. *Int J Pavement Eng* 2021; 1–14. DOI: 10.1080/10298436.2021.1915490.
16. Esmaeli R and Farhad S. Parameters estimation of generalized Maxwell model for SBR and carbon-filled SBR using a direct high-frequency DMA measurement system. *Mech Mater* 2020; 146: 103369.
17. Salimi A, Abbassi-Sourki F, Karrabi M, et al. Investigation on viscoelastic behavior of virgin EPDM/reclaimed rubber blends using Generalized Maxwell Model (GMM). *Polym Test* 2021; 93: 106989.
18. Papagiannakis AT, Abbas A and Masad E. Micromechanical analysis of viscoelastic properties of asphalt concretes. *Transportation Research Record: Journal of the Transportation Research Board* 2002; 1789: 113–120.
19. Flory PJ. Molecular theory of rubber elasticity. *Polym J* 1985; 17: 1–12.
20. Mark JE. Rubber elasticity. *J Chem Educ* 1981; 58: 898–903.
21. Ahagon A, Kida M and Kaidou H. Aging of tire parts during service. I. Types of aging in heavy-duty tires. *Rubber Chem Technol* 1990; 63: 683–697.